ISSN 0965-545X, Polymer Science, Series A, 2017, Vol. 59, No. 1, pp. 53–57. © Pleiades Publishing, Ltd., 2017.
Original Russian Text © K.V. Malafeev, O.A. Moskalyuk, V.E. Yudin, N.G. Sedush, S.N. Chvalun, V.Yu. Elokhovskii, E.N. Popova, E.M. Ivan'kova, 2017, published in Vysokomolekulyarnye Soedineniya, Seriya A, 2017, Vol. 59, No. 1, pp. 47–52.

Synthesis and Properties of Fibers Prepared from Lactic Acid–Glycolic Acid Copolymer

K. V. Malafeev[a, b], **O. A. Moskalyuk**[b, c]*, **V. E. Yudin**[b, d], **N. G. Sedush**[e], **S. N. Chvalun**[e], **V. Yu. Elokhovskii**[b], **E. N. Popova**[b], **and E. M. Ivan'kova**[b]
[a] *St. Petersburg State Technical University, St. Petersburg, 195251 Russia*
[b] *Institute of Macromolecular Compounds, Russian Academy of Sciences, St. Petersburg, 199004 Russia*
[c] *State University of Technology and Design, St. Petersburg, 191186 Russia*
[d] *Kazan (Volga Region) Federal University, Kazan, Tatarstan, 420008 Russia*
[e] *National Research Center Kurchatov Institute, Moscow, 123182 Russia*
**e-mail: olga-moskalyuk@mail.ru*

Received April 25, 2016;
Revised Manuscript Received August 10, 2016

Abstract—A method for preparing laboratory samples of fibers from glycolide-*co*-D,L-lactide to produce bioresorbing suture filaments with a controlled complex of properties is developed. The morphology of fibers obtained through melt spinning is studied. The peculiarities of the mechanical properties of fibers are investigated.

DOI: 10.1134/S0965545X17010096

INTRODUCTION

Polymers and copolymers based on glycolic and lactic acids exhibit some valuable properties, such as biocompatibility and biodegradability, which allows one to predict their wide application in medicine. From these polymers, suture filaments, films of different functional purposes, plates, fasteners for traumatology and orthopedics, and also drugs of prolonged action may be obtained [1–5]. The assortment of such products is growing every year.

Polyglycolide (PGA) has received rather wide acceptance as a suture material. The main advantages of PGA-based suture filaments are high strength approaching the value for polyester fibers and the convenience in use and in sterilization [6, 7]. An essential advantage of the aforementioned suture filaments compared to bioresorbing materials of natural origin, for example, surgical catgut, is also the retention of strength for a longer critical period of time of wound healing (7–11 days) [6]. Moreover, on biodegradation of PGA suture material, no immune reaction of the body is observed, since glycolic acid formed as a result of the polymer degradation is already present in the human body and participates in the natural metabolism [7, 8].

However, the suture materials from PGA have a significant disadvantage, namely, a low elasticity. In the form of monofilament, it can be used only as small-diameter (15–25 μm) products, mainly, in ophthalmology and microsurgery [9]. Thus, to enhance the elasticity of polyglycolide suture filaments and to increase their resolution time in a living organism, the suture materials are made predominantly from lactic acid–glycolic acid copolymer [10]. By varying the chemical composition, molecular mass (MM), and morphology of copolymer, the mechanical properties of the material, its solubility, and the biodegradation time can be controlled [11, 12]. All this in combination with low toxicity, perfect biocompatibility, and bioinertness makes the lactic acid–glycolic acid copolymer a promising material for suture filaments.

The aim of this work was to develop a method for producing laboratory samples of filaments prepared from glycolide–D,L-lactide copolymer and to study their structure as well as stress–strain properties.

MATERIALS AND METHODS OF INVESTIGATION

As the object of investigation, glycolide-D,L-lactide copolymer with molar ratio PGA : PLA = 90 : 10 was used. The copolymer was synthesized in the Laboratory of Polymer Materials of the Kurchatov Complex of NBICS Technologies (National Research Center Kurchatov Institute). Glycolide and D,L-lactide (Corbion, Netherlands) were used without further purification. To a monomer mixture, a solution of tin octanoate in hexane (Aldrich, USA) was added, followed by removal of organic solvent under reduced

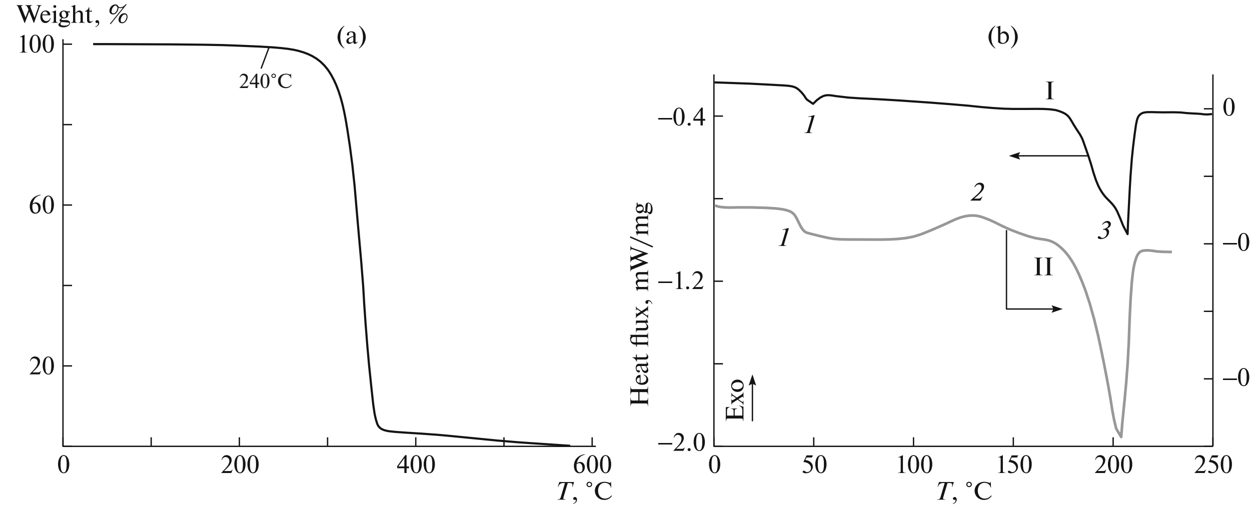

Fig. 1. TGA (a) and DSC (b) curves for PGA–PLA copolymer. (b) (*1*) Glass transition region, (*2*, *3*) crystallization and melting peaks, respectively; (I) first scanning, (II) second scanning.

pressure. The catalyst concentration in the reaction mixture was equal to 200 ppm. As a reactor, a Ceast Smart Rheo 2000 capillary viscometer (Italy) was employed. The polymerization was carried out at 180°C for 3 h. Unreacted polymer was eliminated under vacuum at 200°C for 5 h.

The temperature–time parameters of processing of PGA–PLA copolymer were chosen with the use of thermal and rheological analyses.

The thermal analysis of copolymer was performed by the TGA and DSC methods. The TGA measurements were carried out on a Netzsch TG 209 F1 Iris analyzer (Germany) in an inert medium in the temperature range of 30–600°C at the heating rate of 10 K/min.

The DSC analysis of copolymer was also performed in an inert medium on a Netzsch DSC 204 F1 Phoenix analyzer (temperature range of −80 to +280°C, heating rate of 10 K/min).

The DSC method was used to determine the glass transition temperature, melting temperature, and crystallization temperature of copolymer, with the glass transition temperature measured at the second scanning of the sample.

The rheological study of copolymer was performed on a Physica MCR-301 rheometer (Anton Paar, Austria), with a cone–plane metering unit (25 mm in diameter, angle of 2°). The temperature range of tests was chosen on the basis of the data of TGA and DSC.

PGA–PLA fiber forming was carried out on a DSM Xplore 5 mL Microcompounder double-screw microextruder (DSM Xplore, Netherlands) at the screw rate of 50 min^{-1}, in the range of 210–215°C. At the output from a jet 1 mm in diameter after mixing, the copolymer melt was cooled by a compressed air jet and supplied to intake reels placed at the distance of 260 mm from the jet and rotating at the rate of 20 min^{-1}. Jet stretching was as high as 600%.

The mechanical characteristics of PGA–PLA copolymer fibers prepared from melt were studied on an Instron 5943 tensile test machine. The sample base length was 30 mm and the draw speed was as high as 10 mm/min. From stress-strain diagrams of fiber samples, their strength σ_b, elastic modulus E_0, yield strength σ_y, and elongation at break ε_b were determined.

SEM images of the cryocleavage surface of bioresorbing fibers were recorded on a Carl Zeiss Supra-55 scanning electron microscope (Germany).

X-ray patterns of the samples under investigation were recorded on a DRON-1 X-ray diffractometer (CuK_2 radiation, with a slit collimation). Two slits at the output of the X-ray tube were set up normal to each other; thus, the section of the primary beam was 20 × 20 μm. The sample and a RT-1 X-ray cassette were placed 30 mm apart. The exposure was carried out in a vacuum chamber to reduce the intensity of X-ray scattering in air. The exposure time was 3 h for the PGA–PLA fibers 350 μm thick.

RESULTS AND DISCUSSION

A comprehensive study with the use of TGA, DSC, and rheological analysis making it possible to determine the temperature–time parameters of melt processing of PGA–PLA copolymer was carried out. Figure 1 shows TGA and DSC curves for the initial PGA–PLA granules.

It follows from Fig. 1a that the PGA–PLA copolymer is stable up to 240°C. A further increase in temperature results in thermal degradation of polymer with the successive loss of the sample mass. The relax-

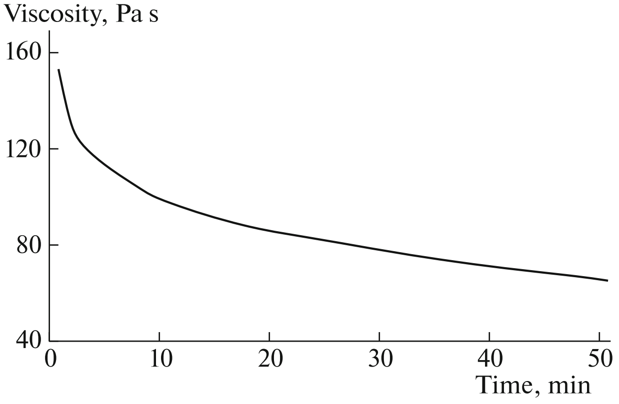

Fig. 2. Time dependence of viscosity of PGA–PLA copolymer melt at 220°C on testing in air.

ation and phase transitions occurring in the copolymer on heating were studied by the DSC method. As can be seen from Fig. 1b, the DSC curve exhibits an inflection at 40°C and two pronounced peaks: an exo peak at 125°C and an endo peak at 205°C. A jump in the heat capacity (inflection) at 40°C is related to glass transition temperature T_g of copolymer. The exo peak at 125°C reflects the additional crystallization of the initial sample caused by an increase in temperature. The endo peak at 205°C is related to the melting temperature of PGA–PLA copolymer, which is in accordance with the published data [11–14].

The development of the method of fiber melt spinning requires the available information on the stability of the fiber rheological characteristics in time. Figure 2 shows the viscosity of PGA–PLA copolymer melt depending on the residence time at 220°C in air. It is evident that, within the first five minutes of the experiment, the copolymer viscosity decreased by 30%, but a value (around 100 Pa s) sufficient for carrying out the fiber melt spinning on a laboratory microextruder was retained. Thus, the residence time of melt in the extruder chamber should not exceed 10 min, and the recommended temperatures of lactic acid–glycolic acid copolymer processing are in the range of 210–215°C.

Further melt spinning of PGA–PLA fibers was carried out on a double-screw microextruder with regard to the set temperature–time parameters of material processing.

The structure of the resulting fibers was studied with the use of scanning electron microscopy, DSC, and X-ray diffraction analysis. The DSC thermogram (Fig. 3, curve *1*) for formed fiber displays an exo maximum in the range of 100–120°C, which was also observed for the initial granules (see Fig. 2b, the first scanning). Thus, it may be assumed that the aforementioned maximum is indicative of the additional crystallization of fiber on its heating in the course of the experiment and, hence, of incomplete crystallization during processing in the microextruder. The endo peak on the DSC curve (Fig. 3, curve *1*) coincides by temperature and heat absorption with the analogous peak for the PGA–PLA initial granules (see Fig. 1b). For fibers, as for granules, the above peak is due to melting of the copolymer crystallites.

To provide the complete crystallization of PGA–PLA fibers prepared on the microextruder, they were subjected to isothermal annealing at 120°C for 10 min. Figures 3 and 4 present the data of DSC and X-ray diffraction analysis, respectively, for such "overcrystallized" samples. On the DSC curve for this sample (Fig. 3, curve *2*), the crystallization peak is absent unlike curve *1* for the initially formed fiber. As is seen from X-ray patterns (Fig. 4), the reflexes in the initially formed fiber are blurred along the circle, and for an annealed sample, intense and narrow reflexes are observed. The latter fact is indicative of the presence of

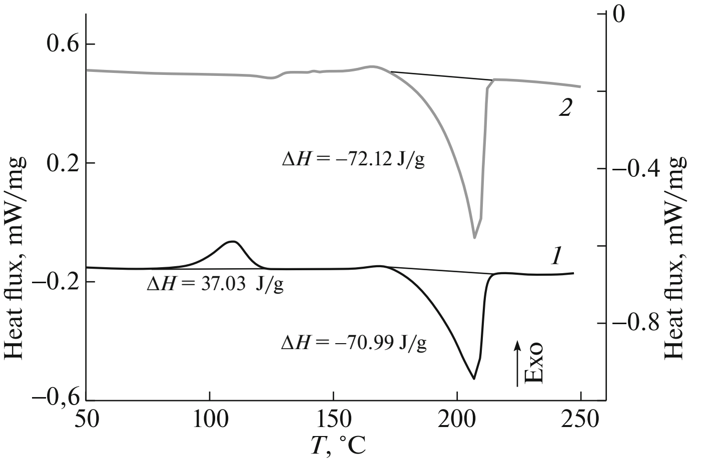

Fig. 3. DSC curves for the initially formed PLA–PGA fiber (*1*, left axis of ordinates) and for crystallized fiber (*2*, right axis of ordinates).

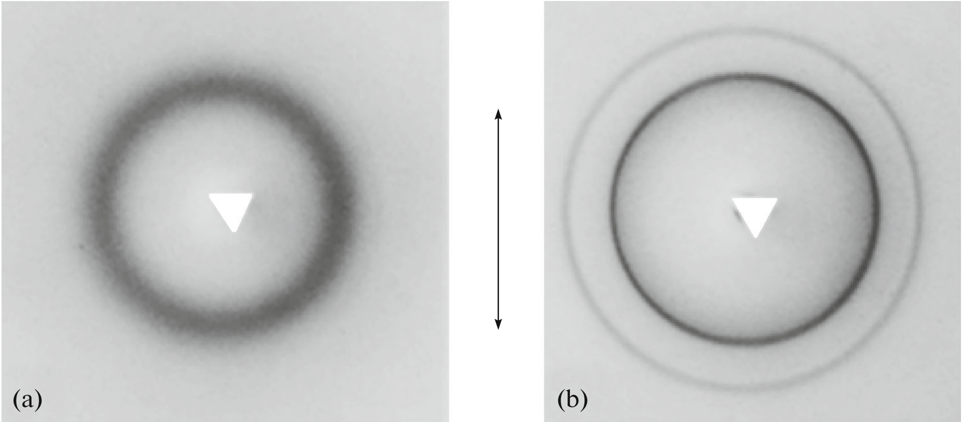

Fig. 4. X-ray patterns of the initially formed PGA–PLA fiber (a) and crystallized fiber (b). The direction of fiber extrusion is shown by arrow.

rather large regions of coherent scattering formed by crystallites with the isotropic arrangement.

The size of crystalline regions of sample of crystallized PGA–PLA copolymer was more thoroughly determined with the use of electron microscopy. Figure 5 shows the SEM image of the surface of transverse cryocleavage of crystallized PGA–PLA fiber. As can be seen, the copolymer structure involves spherulites with the average size of 3–5 μm formed in the course of the isothermal annealing.

The mechanical behavior of the PGA–PLA initially formed fiber and crystallized fiber was analyzed at uniaxial stretching. Figure 6 shows the obtained stress-strain diagrams. As the formed fiber had elongation at break above 100% compared to several percent for crystallized fiber, for reference, the initial portions of diagrams with elongation up to 10% are presented in Fig. 6.

The main mechanical characteristics determined from the stress-strain diagrams are given in the table.

It can be seen from Fig. 6 and the table that the tensile strength and elastic modulus of fibers increase with the content of crystalline phase in fiber. Thus, for the initial fiber, the strength is 45 MPa and the elastic modulus is as high as 3 GPa, whereas for the crystallized sample, σ_b = 80 MPa and E_0 = 4.5 GPa. However, it should be noted that the fiber elasticity decreases significantly with the increase in crystallinity; namely, the deformations at break for the initially formed and crystallized fibers are 140% and less than 10%, respectively. The determined stress-strain characteristics of PGA–PLA fibers correspond to the published data for the class of biodegradable polymers

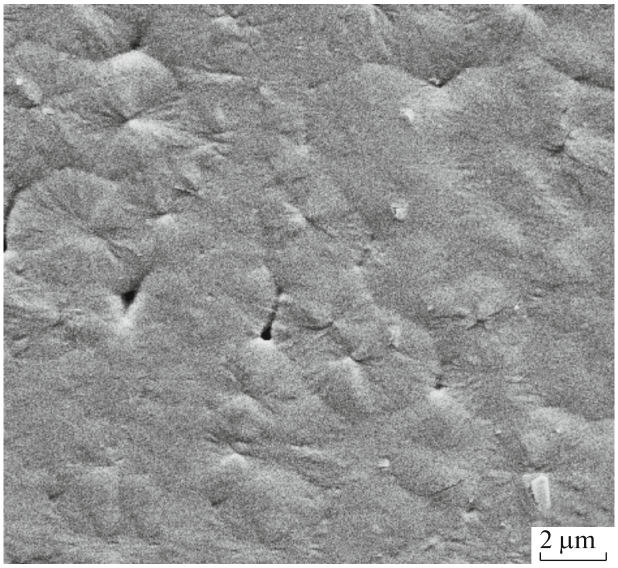

Fig. 5. SEM image of the surface of transverse cryocleavage of crystallized PGA–PLA fiber.

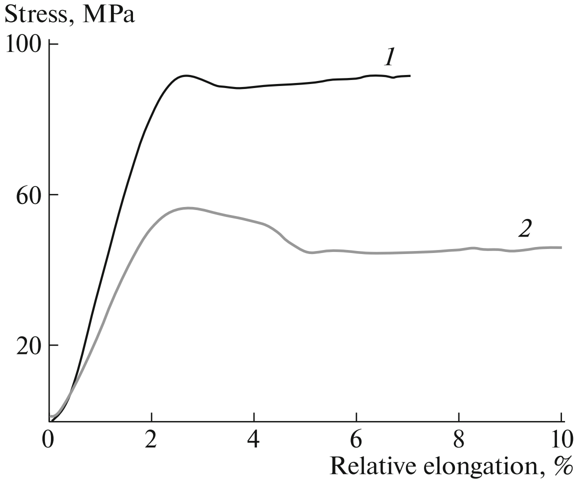

Fig. 6. Stress-strain diagrams of (*1*) crystallized and (*2*) initial PGA–PLA copolymer fibers.

Mechanical properties of PGA–PLA copolymer fibers

Fiber	σ_y, MPa	σ_b, MPa	E_0, GPa	ε_b, %
Initial	62 ± 6	45 ± 5	3.1 ± 0.4	137 ± 12
Crystallized	91 ± 9	80 ± 9	4.5 ± 0.4	7 ± 1

under investigation [15, 16]. Note that the elongation of the initial sample is sufficient for further high-temperature orientation stretching for the purpose of sample strengthening.

CONCLUSIONS

Thus, in this work, the peculiarities of the melt processing technology of bioresorbing copolymer based on lactic and glycolic acids with the content of polylactide of 10% were revealed. The morphology of fiber prepared by melt extrusion was studied. The features of the mechanical properties of PGA–PLA fibers were determined. It was shown that the elongation of the initial fiber prepared by melt extrusion is sufficient to perform further high-temperature orientation stretching for the purpose of producing bioresorbing suture materials with controlled characteristics.

ACKNOWLEDGMENTS

We are grateful to L.P. Myasnikova (Ioffe Physical Technical Institute, RAS) for help in carrying out X-ray diffraction analysis and fruitful discussion.

This work was supported by the Science Foundation of Russia (RNF no. 14-33-00003).

REFERENCES

1. S. Ebnesajjad, *Handbook of Biopolymers and Biodegradable Plastics—Properties, Processing and Applications,* (William Andrew, New York, 2013).
2. R. Jain, Biomaterials **21** (23), 2475 (2000).
3. J. Kreuter, Adv. Drug Delivery Rev. **64**, 213 (2012).
4. R. Dinarvand, N. Sepehri, S. Manoochehri, H. Rouhani, and F. Atyabi, Int. J. Nanomed. **6**, 877 (2011).
5. A. M. Raya-Rivera, D. Esquiliano, R. Fierro-Pastrana, E. López-Bayghen, P. Valencia, R. Ordorica-Flores, S. Soker, J. J. Yoo, and A. Atala, Lancet **384** (9940), 329 (2014).
6. D. N. Bontsevich, Probl. Zdorov'ya Ekol., No. 3, 46 (2005).
7. J. B. Herrmann, R. J. Kelly, and G. A. Higgins, Arch. Surg. (Chicago, IL, U. S.) **100** (4), 486 (1970).
8. *Biocompatible Materials,* Ed. by V. I. Sevast'yanova (Med. informatsionnoe agentstvo, Moscow, 2011) [in Russian].
9. B. G. Belenkaya, V. I. Sakharova, E. A. Sinevich, S. I. Belousov, A. H. Kuptsov, and S. N. Chvalun, Macromol. Symp. **144** (1), 187 (1999).
10. A. A. Kyriacos, G. G. Niederauer, and M. C. Agrawal, Biomaterials **17** (2), 93 (1996).
11. D. W. Grijpma and A. J. Pennings, Macromol. Chem. Phys. **195** (5), 1633 (1994).
12. D. Grijpma, A. Nijenhuis, and A. Pennings, Polymer (Guildf) **31** (11), 2201 (1990).
13. M. Zilberman, Acta Biomater., No. 1, 615 (2005).
14. A. Södergård and M. Stolt, Prog. Polym. Sci. **27** (6), 1123 (2002).
15. X. Yuan and A. F. T. Mak, J. Appl. Polym. Sci. **81**, 251 (2001).
16. A. Cicero John and R. Dorgan John, J. Polym. Environ. **9** (1), 1 (2001).
17. L. Fambri and A. Pegoretti, Polymer **38** (1), 79 (1997).

Translated by L. Tkachenko